Application of a Hybrid Navigation System for an Autonomous Space Air-Launched Vehicle

David Vallverdú, Carles Pou, Mariona Badenas, Eduard Diez

Application of a Hybrid Navigation System for an Autonomous Space Air-Launched Vehicle

David Vallverdú, Carles Pou, Mariona Badenas, Eduard Diez
Space Direction, GTD*
Barcelona, Spain
david.vallverdu@gtd.eu, carles.pou@gtd.eu, mariona.badenas@gtd.eu, eduard.diez@gtd.eu

ABSTRACT

ALTAIR is a European Commission Horizon 2020 project that proposes a space launch system composed of an autonomous aircraft-rocket assembly, dedicated to the market share of small satellites (50-150 kg) in Low Earth Orbit. The rocket, or Space Launch Vehicle (SLV), comprises a cost-effective lightweight navigation system that fuses Global Navigation Satellite System (GNSS) data and readings from an Inertial Measurement Unit (IMU). The combination of these two technologies allows for a significant cut of the system mass budget with respect to traditional inertial-only navigation systems, without consequential accuracy loss. Additionally, ALTAIR embeds the alignment process on-board the SLV, which is performed during captive flight. Transferring this task to after take-off significantly simplifies ground operations in terms of both time and safety, hence further decreasing the cost of each launch campaign.

This paper is divided into two parts: navigation performance assessment and its application for autonomous on-board safety algorithms. First, it presents the sensor fusion algorithm used to hybridize GNSS and IMU during the SLV free flight, including the captive alignment process. It describes a loosely coupled architecture of the hybrid navigation system, which combines a profile-free alignment with a profile-based GNSS/IMU data fusion. It then analyses the performance of this implementation that uses the Indirect (error-based) and Extended Kalman filters. Second, it evaluates the impact of sensor fusion on the safety algorithms that assess the nominal launcher state and engine failure free-fall scenario. Results show that hybrid navigation can be used to maintain a bounded error navigation solution throughout the in-flight initialization, the alignment manoeuvre and the free fall before ignition. Furthermore, transfer-alignment previous to SLV release prevents transient errors during the most critical initial seconds of free flight.

Keywords— airborne launcher; nanosatellites; avionics; embedded systems; hybrid navigation; Kalman filter; indirect Kalman filter; Unscented transform; in-flight alignment

I. INTRODUCTION

The space sector worldwide is undergoing deep changes in terms of client needs and potential services offered; it observes trends such as bigger constellations of smaller satellites, a higher use of Commercial off-the-Shelf (COTS) hardware, a growth of multidisciplinary space projects, and rising environmental awareness [1], [2]. Several telecommunications providers (*e.g.* OneWeb) or Earth observation initiatives (*e.g.* Planet Lab's Dove) exemplify the new interest for highly populated small-satellite Low Earth Orbit (LEO) constellations. Small satellite missions have traditionally been served by heavy launchers, including Ariane 5, Soyuz or Proton M [3]. These services, however, are not optimal for injection and maintenance tasks dedicated to this type of payloads, especially at the high launch rates that these new projects require [4].

It is from this new demand that ALTAIR[1] is born. A Horizon 2020 project, ALTAIR proposes a new concept of a fully autonomous launch system aimed at placing small satellites (50-150 kg) into LEO. It seeks economic viability through cost-effective high launch rates, while ensuring mission flexibility for different payload needs and a low environmental impact. To this end, efforts are focused along two lines. First, the equipment mass is reduced by using COTS and discharging hardware functions to the on-board software. Secondly, the costs are decreased by shortening and simplifying the ground operations and increasing the

*Partner of the ALTAIR consortium, funded by the European Commission Horizon 2020 program under agreement No 685963.

[1]ALTAIR stands for "Air Launch space Transportation using an Automated aircraft and an Innovative Rocket."

software missionization. This paper demonstrates that the navigation and safety algorithms embedded on-board using this approach do not reduce the safety of the mission.

The ALTAIR concept consists of a first stage autonomous carrier aircraft that, at high altitude, deploys a lightweight rocket, or Space Launch Vehicle (SLV), carrying the payload. The scope of the project also comprises the feasibility study of the ground segment and its operations. The use of a carrier allows the SLV to stay inactive on ground, increasing safety and alleviating further operational overheads. Furthermore, this mission approach allows for shorter campaigns and greater flexibility, which result in simplified and faster operations on ground ranging from safety assessment to the SLV assembly.

As a fully autonomous concept, ALTAIR embedded systems have a key role in the design of the SLV; indeed, tasks that are typically performed on ground and are transferred to on-board avionics. In line with ALTAIR's approach, modular and configurable embedded systems based on COTS hardware are of high interest. Modularity eases assembly operations and validation tasks and the use of COTS diminishes the risk of campaign halts due to specialized provider failure. In addition, given that the SLV is not active on ground, its avionics need to be initialized during captive flight when the SLV is still attached to the carrier. This introduces a set of new challenges unseen in conventional launchers.

This paper assesses the performance of the navigation algorithms and their impact on the safety algorithms used to guarantee the proper release of the SLV from the carrier. This separation is one of the most critical phases of the mission due to its strict safety constraints and the lack of active control mechanisms for the SLV's attitude. In particular, the navigation scenario studied in this paper consists of an initialization during carried flight, followed by a release manoeuvre and a short free fall. Fig. 1 illustrates the evolution of the navigation and safety requirements along the mission.

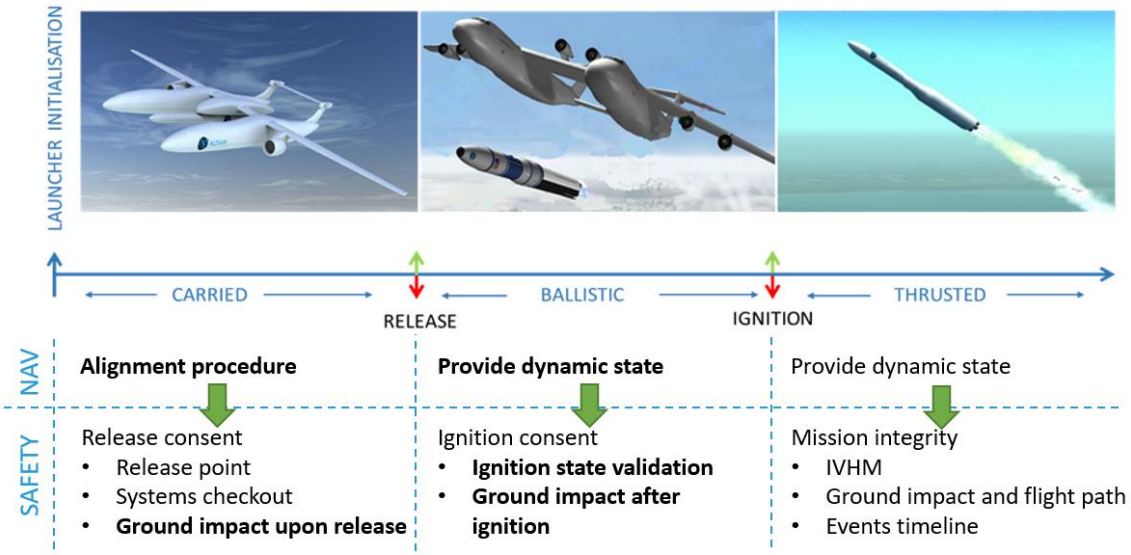

Fig. 1. Navigation and Safety requirements during the ALTAIR mission. This paper studies the ones highlighted in bold.

Available instruments are a low-cost GNSS sensor and an Inertial Measurement Unit (IMU). It has been proven that GNSS/IMU hybrid navigation algorithms can perform acceptably on a typical launch environment such as ORION (with barometer sensors) [5] or SHEFEX-2 (with star tracker) [6], as well as aeronautic (with magnetometers) [7] or land [8] scenarios. The in-flight alignment of inertial navigation systems is covered in the field of missiles [9], [10].

The following section provides an overview of the design architecture of the navigation system. Section III explains the purpose of the safety assessment algorithms. Section IV studies the expected performance of the navigation subsystem and analyses the effect on the reliability of the safety algorithms. Finally, Section V summarizes the findings and conclusions of this work.

II. NAVIGATION SUBSYSTEM

This paper focuses on the design challenges of the ALTAIR SLV navigation system. The navigation system of current launch vehicles, such as Ariane 5 and VEGA, integrate inertial measurements along the mission timespan to obtain the navigation state of the vehicle [11], [12]. Due to integration, IMU-only navigation accumulates errors that grow unbounded over time. Thus, these systems require high-end IMUs with very low noise and biases [13]. This results in significantly massive hardware, at a high cost relative to the mass budget of the vehicle.

Following the low cost COTS guideline, the ALTAIR SLV uses hybrid navigation, fusing data from a low-end Inertial Measurement Unit (IMU) and a Global Navigation Satellite System (GNSS). Because the embedded systems of the SLV boot up during captive flight, a transfer alignment is needed to initialize the hybrid navigation [13], [14]. Fig. 2 shows the resulting architecture. The two navigation modules have different prominence depending on the phase of the mission:

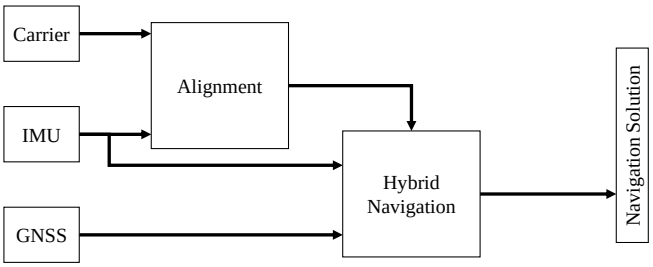

Fig. 2. Navigation architecture

- During captive flight, after avionics initialization, the SLV uses carrier navigation data and its own IMU to align its navigation.
- Upon release of the SLV from the carrier, the alignment module transfers the aligned navigation state to the hybrid navigation module.
- After SLV release, the already initialized hybrid navigation continuously provides a navigation solution by hybridizing on-board IMU and GNSS sensors.

Main hybrid navigation techniques involve the use of Kalman filters. They can be divided into profile-based and profile-free. On the one hand, profile-based implementations use a dynamic state model that increases the accuracy of the estimation when the vehicle trajectory fits the model, but fail when it does not. On the other hand, profile-free implementations make no assumptions on the type of trajectory that the vehicle follows –this approach can be used for a wider range of trajectories, but performs worse than a well matched profile-based method of the same computational order. The potential navigation filters considered for use in the SLV are a profile-free Extended Kalman Filter (EKF) [15] and a profile-free Indirect Kalman Filter (IKF) [13] that uses a linearized state-error model.

A. Alignment

Alignment is the process by which the initial state (position, velocity and attitude) of an inertial navigation system is determined [13]. This is most critical in IMU-only systems, in which alignment errors can totally define their performance throughout the whole mission. The SLV hybrid navigation system can absorb some initial error thanks to GNSS measurements, at the cost of a transient phase in which navigation errors are above nominal level. However, while the SLV is captive, GNSS signal may be unavailable due to carrier interference. Therefore, a transfer-alignment process before release is still desirable so that pre-release safety assessment algorithms have accurate navigation data at their disposal –these are the most critical users of the navigation output.

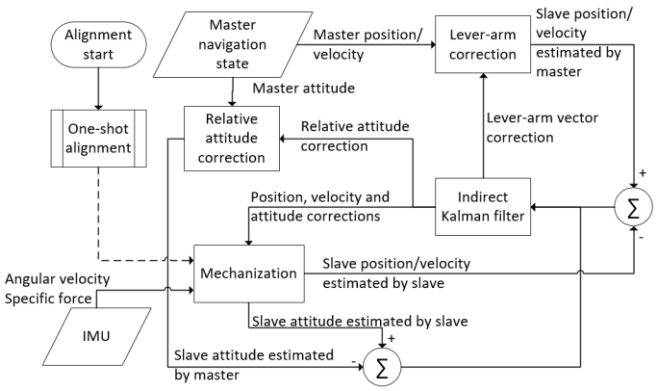

Fig. 3. Transfer alignment diagram starting from (dotted line) a one-shot initialization of the Mechanization process (i.e. rough copy of the master navigation state at initialization time)

Given that SLV embedded systems initialize during captive flight, alignment happens in a non-stationary environment. The strategy used, known as transfer alignment, involves the carrier (*aka* master) transferring its own navigation data to the SLV (*aka* slave) during captive flight (See Fig. 3). For this data transfer to be useful for SLV alignment purposes, the carrier simultaneously needs to perform a certain manoeuvre that dynamically stimulates the IMU on-board the SLV. A profile-free Indirect Kalman Filter (IKF) [13] matches carrier navigation data (position, velocity, attitude or a combination of these) with SLV IMU measurements via a linearized model of the alignment error.

B. Hybrid Navigation

Upon release of the SLV, the navigation solution provided by the alignment process is transferred to the hybrid navigation module, which fuses data from IMU and GNSS sensors to continue to provide a reliable navigation solution without transient errors. Fig. 4 depicts this process. An Extended Kalman Filter (EKF) is used to continuously update the navigation solution, which becomes available to all navigation users (e.g. safety algorithms, GNC, telemetry, etc.).

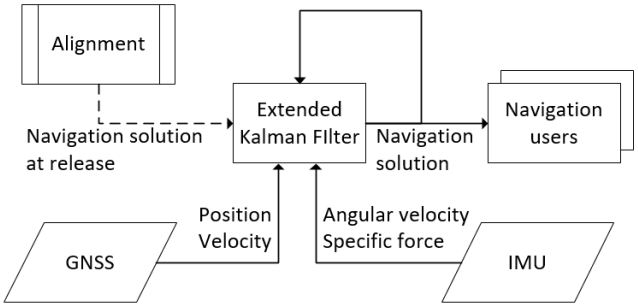

Fig. 4. Hybrid navigation diagram initializing the EKF with the alignment navigation solution (dotted line).

The state of the EKF is given by

$$\vec{x} = \left[\vec{r}^{i^T} \quad \vec{v}^{i^T} \quad f^{i^T} \quad \vec{\omega}_{ib}^{b\ T} \quad \Psi_i^{b^T}\right]^T ,$$

where $\vec{r}^i$ and $\vec{v}^i$ are respectively the position and velocity of the SLV in the ECI frame, f^i is the specific force[2] received by the SLV (also in ECI), $\vec{\omega}_{ib}^{b\ T}$ is the angular velocity expressed in the body frame (attached to the SLV) of the SLV around ECI, and Ψ_i^b represents the 3-2-1 Euler angles that transform from ECI to the body frame. The EKF propagates the state from one time-step to the next with the model:

$$\vec{r}^i(t+\Delta t) = \vec{r}^i(t) + \vec{v}^i(t)\Delta t + \left(\vec{f}^i(t) + \vec{g}^i(t)\right)\frac{\Delta t^2}{2} ;$$

$$\vec{v}^i(t+\Delta t) = \vec{v}^i(t) + \left(\vec{f}^i(t) + \vec{g}^i(t)\right)\Delta t ;$$

$$\vec{f}^i(t+\Delta t) = \vec{f}^i(t) ; \vec{\omega}_{ib}^b(t+\Delta t) = \vec{\omega}_{ib}^b(t) ;$$

$$\vec{\Psi}_i^b(t+\Delta t) = \vec{\Psi}_i^b(t) + \Delta t \begin{bmatrix} \omega_x + \left(\sin\phi\,\omega_y + \cos\phi\,\omega_z\right)\tan\theta \\ \left(\cos\phi\,\omega_y - \sin\phi\,\omega_z\right) \\ \left(\sin\phi\,\omega_y + \cos\phi\,\omega_z\right)\sec\theta \end{bmatrix}.$$

The following notation has been used: $\vec{\omega}_{ib}^b(t) = [\omega_x \quad \omega_y \quad \omega_y]$ and $\vec{\Psi}_i^b(t) = [\phi \quad \theta \quad \psi]$. The measurement model estimates the IMU and GNSS measurements from the state as:

$$\vec{r}_{GPS}^i = r^i ; \vec{v}_{GPS}^i = v^i ; \vec{f}_{IMU}^b = C_i^b \vec{f}^i ; \vec{\omega}_{ib_{IMU}}^b = \vec{\omega}_{ib}^b .$$

Note that the matrix C_i^b is the rotation matrix from ECI to body frame, which can be calculated from Ψ_i^b [13].

III. Operational Impact: On-Board Flight Safety

The on-board safety system ensures the protection of people and goods through all the phases of the mission. Its role is especially crucial during release, when the SLV performs a short free-uncontrolled flight. During this stage, the navigation solution is used on-board the SLV by two real-time safety algorithms, illustrated in the safety architecture of Fig. 5.

The first algorithm, identified as the Ground Safety Analyser, estimates the impact area on ground under the hypothesis that the SLV performs a ballistic fall after release. Then, the Safety Criteria Evaluator algorithm compares this information to an on-board sensitive area database (e.g. populated regions, etc.) and decides whether it is safe to authorise release.

At release and during subsequent free-fall, the second algorithm, the Flight Safety Analyser, predicts the attitude of the SLV at nominal ignition time. In parallel, the Safety Criteria Evaluator compares this predicted attitude to the attitude that the SLV should have for a nominal ignition. In the event that the difference is outside acceptable mission margins, the Safety Evaluator requests Ground Control to inhibit ignition.

[2] Specific force is the acceleration due to non-conservative forces, such as thrust, aerodynamic loads, etc..

A. Flight Safety Analyser

The Flight Safety Analyser (FSA) uses the navigation solution (i.e. position, velocity and attitude) and the angular velocity computed by the gyroscope to predict the attitude in the near future. To this end, the FSA propagates the state

$$\vec{x} = \begin{bmatrix} \vec{r}^{\,i\,T} & (d\vec{r}^{\,i}/dt)^T & \vec{q}_b^{\,i\,T} & \vec{\omega}_{ib}^{\,b\,T} \end{bmatrix}^T$$

through time by integrating the system

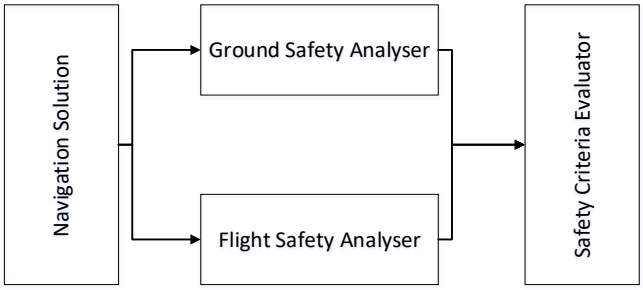

Fig. 5 Illustrative on-board safety architecture.

$$\frac{d\vec{x}}{dt} = \left[\left(\frac{d\vec{r}^{\,i}}{dt}\right)^T \quad \left(\frac{\vec{F}_a^{\,i}}{m} - \frac{\mu}{\|\vec{r}^{\,i}\|^3}\vec{r}^{\,i}\right)^T \quad \left(\frac{1}{2}\boldsymbol{\Omega}\vec{q}_b^{\,i}\right)^T \quad \left(\boldsymbol{I}^{-1}\left(\sum\vec{M}_{CG} - \vec{\omega}_{ib}^{\,b} \times \left(\boldsymbol{I}\vec{\omega}_{ib}^{\,b}\right)\right)\right)^T \right]^T$$

using a classic Runge-Kutta of order 4 (RK4) [18]. In the above equation, t is time, μ is the Earth's gravitational constant, $\vec{r}^{\,i}$ is the position of the SLV in Earth Centred Inertial (ECI) frame, $\vec{q}_b^{\,i}$ is the quaternion[3] that transforms from body frame (attached to the SLV) to ECI frame, $\vec{\omega}_{ib}^{\,b}$ is the angular velocity of the SLV around ECI in body frame, $\boldsymbol{I}$ is the inertia tensor of the SLV in body-frame, $\boldsymbol{\Omega}$ is the quaternion multiplication matrix

$$\boldsymbol{\Omega} = \begin{bmatrix} -\left[\vec{\omega}_{ib}^{\,b} \times\right] & -\vec{\omega}_{ib}^{\,b} \\ \vec{\omega}_{ib}^{\,b\,T} & 0 \end{bmatrix}$$

used to compute the variation of the quaternion with time [19], [20], and $\vec{F}_a^{\,i}$ and $\sum\vec{M}_{CG}$ are respectively the aerodynamic force and torque experienced by the SLV in its centre of gravity (CG). The latter are function of velocity, as well as of the geometric characteristics of the launcher (i.e. lift and drag coefficient, distance from CG to centre of pressure CP, cross-section area and fin area).

B. Ground Safety Analyser

The Ground Safety Analyser (GSA) uses the navigation position and velocity to predict the point on the Earth's surface where the launcher would fall should it not ignite after release –i.e. in case it performed a free fall. This point is used afterwards to compute an impact area, by including the uncertainties of the model. Because this propagation occurs much farther away in the future than the FSA, the GSA does not propagate attitude, and does not use RK4. Instead, the propagator is an expansion of the F&G Series [22]. This method is based on the Taylor decomposition of

$$\vec{r}^{\,i}(t + \Delta t) = \sum_{n=0}^{+\infty} \frac{\Delta t^n}{n!} \frac{d^n\vec{r}^{\,i}}{dt^n}\bigg|_{t_0}$$

and the fact that each term of the Taylor series can be expressed as

$$\frac{1}{n!}\frac{d^n\vec{r}^{\,i}}{dt^n} = f_n\vec{r}^{\,i} + g_n\frac{d\vec{r}^{\,i}}{dt} + h_n\vec{v}^{\,i} + i_n\frac{d\vec{w}^{\,i}}{dz},$$

where

$$\vec{v}^{\,i} = \frac{d\vec{r}^{\,i}}{dt} - \vec{\Omega}_E^{\,i} \times \vec{r}^{\,i} - \vec{w}^{\,i}$$

is the velocity of the SLV relative to the air in ECI, $\vec{\Omega}_E^{\,i}$ is the inertial angular rotation of the Earth in ECI, $\vec{w}^{\,i}$ is the wind speed relative to the Earth in ECI, and z is the altitude of the SLV. The wind speed depends only on the altitude, and any model shall be used. The coefficients f_n, g_n, h_n and i_n for $n \geq 2$ can be deduced by derivation of the dynamic model

[3] By convention in this paper, quaternions expressed in vector form $\vec{q} = [q_1 \quad q_2 \quad q_3 \quad q_4]^T$ correspond to the hypercomplex number $\boldsymbol{q} = q_4 + q_1\boldsymbol{i} + q_2\boldsymbol{j} + q_3\boldsymbol{k}$, where $\boldsymbol{i}^2 = \boldsymbol{j}^2 = \boldsymbol{k}^2 = -1$, $\boldsymbol{ij} = -\boldsymbol{ji} = \boldsymbol{k}$, $\boldsymbol{jk} = -\boldsymbol{kj} = \boldsymbol{i}$ and $\boldsymbol{ki} = -\boldsymbol{ik} = \boldsymbol{j}$. Likewise, a rotation quaternion $\boldsymbol{q}_a^b$ in vector form is $\vec{q}_a^{\,b} = [(\vec{e}\sin(\phi/2))^T \quad \cos(\phi/2)]$, being $\vec{e}$ and ϕ the Euler axis-angle [13] equivalent rotation from frame a to frame b.

$$\frac{d^2\vec{r}^i}{dt^2} = \left(\frac{d^2\vec{r}^i}{dt^2}\right)_G + \left(\frac{d^2\vec{r}^i}{dt^2}\right)_A = -\frac{\mu}{\|\vec{r}^i\|^3}\vec{r}^i - \frac{\rho\|\vec{v}^i\|}{2\beta}\vec{v}^i \,.$$

Here, β is the SLV ballistic coefficient and ρ is the air density. Thus, the position can be propagated by using

$$\vec{r}^i(t_0 + \Delta t) = f\vec{r}^i + g\frac{d\vec{r}^i}{dt} + h\vec{v}^i + i\frac{d\vec{w}^i}{dz} \text{ and}$$

$$\frac{d\vec{r}^i}{dt}(t_0 + \Delta t) = \frac{df}{d\Delta t}\vec{r}^i + \frac{dg}{d\Delta t}\frac{d\vec{r}^i}{dt} + \frac{dh}{d\Delta t}\vec{v}^i + \frac{di}{d\Delta t}\frac{d\vec{w}^i}{dz},$$

where

$$f = \sum_{n=0}^{+\infty} f_n \Delta t^n \,;\; g = \sum_{n=0}^{+\infty} g_n \Delta t^n \,;\; h = \sum_{n=0}^{+\infty} h_n \Delta t^n \,; i = \sum_{n=0}^{+\infty} i_n \Delta t^n \,.$$

IV. Results

The four algorithms explained in the previous sections have been tested on the scenario presented in Tab. 1. Within this scenario, the position and velocity RMS errors used to corrupt the GNSS measurements depend both on the satellite constellation –more precisely, location and number of available satellites – and on atmospheric conditions [16]. The test scenario simulates the 24-satellite GPS constellation. The atmospheric conditions correspond to the standard published in Solimeno [17].

Tab. 1 Minimum, maximum and nominal values of the parameter-set that describes the test scenario.

Parameter	**Minimum**	**Maximum**	**Nominal**
Air speed			250 m/s
Cruise altitude			10 km
Alignment manoeuvre duration	20 s	30 s	25 s
Maximum carrier roll acceleration			120 deg/s^2
Maximum carrier load factor			3
Carrier update frequency	1 Hz	100 Hz	10 Hz
Carrier position RMS	10 m	1000 m	10 m
Carrier velocity RMS	1 m/s	100 m/s	1 m/s
Carrier attitude RMS	0.1 deg	10 deg	0.1 deg
Carrier-SLV relative attitude RMS			1 deg
SLV Ignition time (after release)		20 s	10 s
IMU update frequency	100 Hz	400 Hz	100 Hz
IMU Accelerometer RMS	2E-3 m/s^2	2E-1 m/s^2	2E-3 m/s^2
IMU Gyroscope RMS	6E-2 deg/s	6 deg/s	6E-2 deg/s
GNSS update frequency			1 Hz
SLV mass			40E3 kg
SLV moment of inertia in longitudinal axis			3E3 kg·m^2
SLV moment of inertia perpendicular to longitudinal axis			2E5 kg·m^2
SLV products of inertia			0
Position of CP relative to CG in longitudinal axis			1 m behind

The four algorithms are run in *cascade* mode, all on the same scenario: the hybrid navigation algorithm is initialized with the alignment output, and the two safety algorithms use navigation data as an input.

A. Navigation Alignment

To assess the feasibility of an in-flight initialization of the ALTAIR hybrid navigation system as well as the sensitivity of the different methods used, several alignment simulations are performed within a range of representative scenarios. Each scenario combines:

- Type of alignment: this depends entirely on the type of data available from the carrier. The simulations test position matching, velocity matching, attitude matching, and all the possible 2- and 3-combinations [13], [14] of these.

- Manoeuvre performed by the carrier: from less to more aggressive manoeuvre, tests include straight flight (no manoeuvre), wing rock (roll oscillations), coordinated turn, and Thach weave (a series of coordinated turns) [14].

To assess filter accuracy, the test consists of a 100 repetitions Monte Carlo scenario, from which the RMS of the actual error can be compared to the RMS predicted by the alignment filter on one repetition. Simulation results (Fig. 6) prove that aggressive manoeuvres combined with full state matching give best alignment performances. This is especially true for yaw estimation, which is the less connected state to position and velocity measurements.

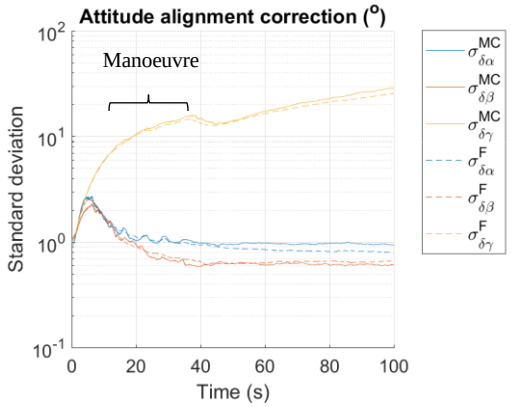

Fig. 6.a) Velocity matching – wing rock.

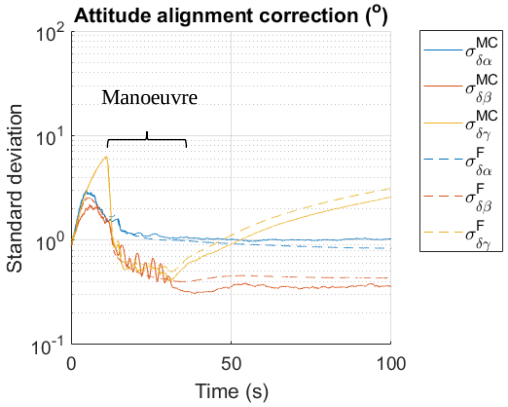

Fig. 6.b) Velocity matching – Thach weave.

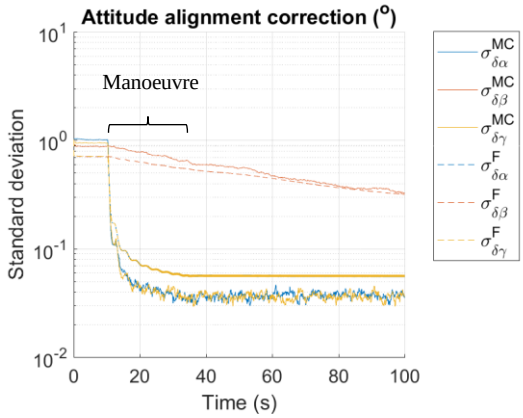

Fig. 6.c) Position + Velocity + Attitude matching – wing rock.

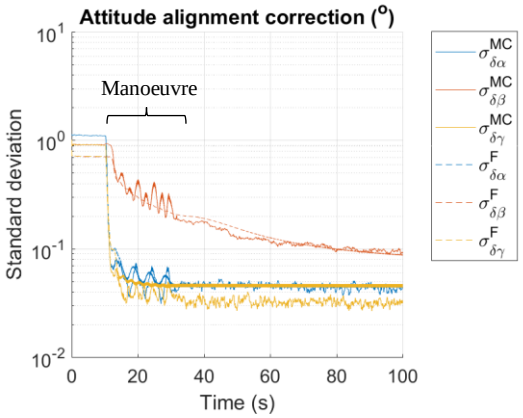

Fig. 6.d) Position + Velocity + Attitude matching – Thach weave.

Fig. 6. Attitude alignment error RMS from Monte-Carlo simulation ($\boldsymbol{\sigma_{\delta x}^{MC}}$) and one filter run ($\boldsymbol{\sigma_{\delta x}^{F}}$). $\delta\alpha$, $\delta\beta$ and $\delta\gamma$ are roll, pitch and yaw errors in the North-East-Down frame, respectively.

Further sensitivity studies have been performed on the quality of the IMU sensors and the carrier navigation data. No tests have been performed to understand the correlated effect of increasing both IMU and carrier RMS error at the same time. The results, presented in Tab. 2, show that the alignment algorithm is most sensitive to carrier data quality, and is rather robust against IMU degradation.

These initial seconds of free flight, when the SLV performs an uncontrolled ballistic fall until ignition, are most critical in terms of safety assessment, which uses the navigation solution as an input. The fact that an accurate and stable navigation solution can be guaranteed since release adds confidence to these safety-related diagnostics.

Tab. 2 Error in velocity, attitude and position 60 s after the manoeuvre ends, in a Thach weave and Position + Velocity + Attitude Matching. Degraded values in bold.

Scenario	**Input**		**Output**		
	IMU RMS scale factor	Carrier RMS scale factor	Navigation position RMS [m]	Navigation velocity RMS [m/s]	Navigation attitude RMS [deg]
Nominal	1	1	1	0.1	0.1
Degraded IMU	**100**	1	2	0.5	1
Degraded Carrier	1	**100**	100	10	2

B. Hyrbrid Navigation

The hybrid navigation test scenario follows that of the alignment scenario. That is, the SLV performs a free fall after the release is executed. The EKF is initialized with the alignment RMS errors presented in Tab. 2 (nominal): 1 m, 0.1 m/s and 0.1 deg in position, velocity and attitude respectively. The results of the test, evaluated in a 100 repetitions Monte Carlo simulation, are shown in Fig. 7.

The simulation results illustrate that the final RMS error of the alignment remains constant during the subsequent hybrid navigation, which takes place upon release. As can be observed, the velocity RMS error estimated by the filter increases slightly in between GNSS updates; this is likely due to the accumulation of IMU integration errors. Nonetheless, each GNSS update corrects it enough to keep the RMS error stable in the long term. In terms of attitude, the RMS error estimated by the filter corresponds to the real RMS error computed with the Monte Carlo method. Although not included in Fig. 7, position RMS error has a similar behaviour to that of velocity: degradation due to IMU is palliated by GNSS updates, so that the RMS error stays at 1 m in the long run.

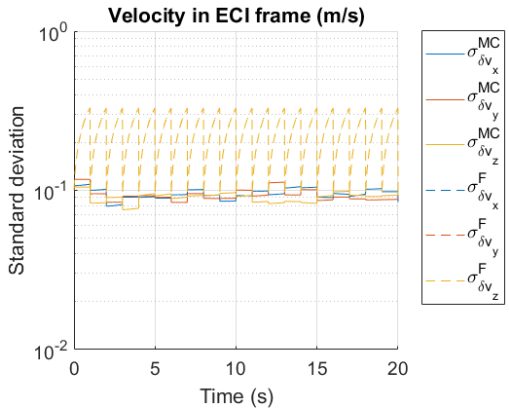

Fig. 7.a) Velocity RMS error.

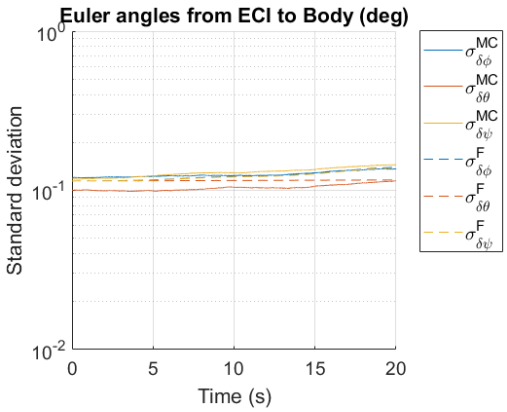

Fig. 7.b) Attitude RMS error.

Fig. 7. Hybrid navigation RMS error from Monte-Carlo simulation ($\boldsymbol{\sigma_{\delta x}^{MC}}$) and one filter run ($\boldsymbol{\sigma_{\delta x}^{F}}$), during free fall after release.

These results confirm that the navigation architecture of ALTAIR (Fig. 2), which implements conventional and well-established Kalman filtering adapted to the ALTAIR scenario, is able to provide a stable and low RMS error navigation solution during the most critical phase of the mission: the SLV release. Overall, this implementation delivers a navigation solution with RMS errors similar to those of inertial navigation systems embedded on legacy launchers [11], [12], but using COTS IMUs instead of highest quality ones.

C. In-flight Safety

To test the in-flight safety algorithm against the navigation accuracy, the FSA is run within an unscented transform (UT) [21] envelope, applied to the scenario at SLV release presented in the previous section – that is, taking as an input the navigation covariance predicted by the navigation filter (as well as the covariance associated to the gyroscope error for $\vec{\omega}_{ib}^{b}$). The predicted attitude RMS error due to release navigation error is shown in Tab. 3.

These results show that the error in the predicted attitude is mainly affected by the quality of input velocity and attitude. This is expected given that the error in initial attitude directly affects error in output attitude and, at the same time, the aerodynamic torques that govern attitude depend mainly on velocity. However, position has little influence on the torques that control the attitude (note that gravity does not

change significantly over several hundreds of meters). All in all, degraded navigation errors of 1 m/s and 1 deg RMS contribute to the predicted attitude uncertainty with about 1 deg RMS error.

Tab. 3 Error in attitude 10 s into the future predicted at release time, with a RK4 time-step of 0.5 s. Degraded values in bold.

Scenario	**Input**			**Output**	
	Navigation position RMS at release [m]	Navigation velocity RMS at release [m/s]	Navigation attitude RMS at release [deg]	Predicted roll RMS [deg]	Predicted pitch/yaw RMS [deg]
Nominal	1	0.1	0.1	1	0.15
Degraded Generic x10	**10**	**1**	**1**	1.6	1
Degraded Generic x100	**100**	**10**	**10**	12	10
Degraded Position	**100**	0.1	0.1	1	0.15
Degraded Velocity	1	**10**	0.1	2	4.5
Degraded Attitude	1	0.1	**10**	12	10

D. Ground Safety Analyser

A similar test to that of the FSA is performed for the GSA. Within a UT envelope, an impact point is propagated from the navigation scenario at release (presented in Tab. 2). With an adaptive time-step, determinism is ensured by establishing a maximum number of iterations and propagation time. For this test, the f, g, h and i coefficients have been computed with contributions of gravity (G) to the dynamic model up to order 4 and aerodynamics (A) up to order 3. Wind speed is considered to be zero throughout the fall.[4] Impact point RMS error due to release navigation error is shown in Tab. 4.

Tab. 4 Error in impact point predicted at release time, with a maximum time-step of 0.2 s. Bold values indicate different than nominal.

Scenario	**Input**		**Output**
	Navigation position RMS at release [m]	Navigation velocity RMS at release [m/s]	Predicted impact point RMS [m]
Nominal	1	0.1	3
Degraded Generic x10	**10**	**1**	30
Degraded Generic x100	**100**	**10**	300
Degraded Position	**100**	0.1	100
Degraded Velocity	1	**10**	250

The intrinsic error associated to the F&G propagation method, when applied from 10 km altitude, has an error RMS of 100 m at the impact point. Thus, the contribution of nominal navigation error RMS of 1 m and 0.1 m/s to impact error is negligible. In terms of GSA sensitivity relative to the navigation input accuracy, while navigation position error RMS is propagated "as is" to the impact point, navigation velocity error RMS has a strong influence on the final impact point RMS error.

V. CONCLUSION

The results obtained in this study show that the performance of COTS-based hybrid navigation systems initialized in-flight matches the navigation requirements of conventional launch vehicles using only inertial navigation. Furthermore, the navigation solution is fully available for on-board autonomous safety assessment and in-flight decision-making during the most critical phases of the mission.

This paper shows that two aspects improve the economic feasibility of the ALTAIR concept. On the one hand, the navigation performance in both nominal and degraded cases does not detriment the performance of the two on-board safety algorithms, thus allowing for the use of COTS. On the other hand, embedding the in-flight navigation initialization and on-board safety results in a simplification of ground operations. To sum up, a feasible low-cost navigation takes ALTAIR one step closer to its goals, and opens the door to a wide range of possibilities within the small-satellite launch systems market.

The next step for the ALTAIR avionics is to validate the obtained navigation performances with the whole set of safety and GNC requirements of the project. To this end, the navigation system simulated in this paper will be tested on real-time flight next year. Additionally, current work is considering the use of

[4] Sensitivity studies of the GSA to wind speed is outside the scope of this paper.

alternative data fusion filters including the Unscented Kalman Filter (UKF) and the implementation of profile-free models during hybrid navigation.

REFERENCES

[1] J. Foust, "Emerging Opportunities for Low-Cost Small satellites and Commercial Space," in *24th Annual AIAA/USU - Conference on small satellites*, 2010.

[2] B. Doncaster, C. Williams, and J. Shulman, "Small Satellite Report: 2017 Nano/Microsatellite Market Forecast," SpaceWorks Enterprises, Atlanta, GA, USA, 2017.

[3] S. J. Isakowitz, J. B. Hopkins, and J. P. Hokpins Jr., *International Reference Guide To Space Launch Systems*, 4th ed. Reston, VA, USA: American Institute of Aeronautics and Astronautics, 2004.

[4] M. S. Hubbard *et al.*, "Growing the Future of Commercial Space," *New Sp.*, vol. 1, no. 1, pp. 3–9, 2013.

[5] R. S. Gay, G. N. Holt, and R. Zanetti, "Orion Exploration Flight Test-1 Navigation Performance Assessment Relative To the Best Estimated Trajectory," in *39th Annual AAS Guidance, Navigation & Control Conference*, 2016.

[6] S. R. Steffes, "Development and Analysis of SHEFEX-2 Hybrid Navigation System Experiment," Techinsche Universität München, 2013.

[7] J. Bijker and W. Steyn, "Kalman filter configurations for a low-cost loosely integrated inertial navigation system on an airship," *Control Eng. Pract.*, vol. 16, no. 12, pp. 1509–1518, Dec. 2008.

[8] Y. Liu, X. Fan, C. Lv, J. Wu, L. Li, and D. Ding, "An innovative information fusion method with adaptive Kalman filter for integrated INS/GPS navigation of autonomous vehicles," *Mech. Syst. Signal Process.*, vol. 100, pp. 605–616, Feb. 2018.

[9] H. Chu, T. Sun, B. Zhang, H. Zhang, and Y. Chen, "Rapid Transfer Alignment of MEMS SINS Based on Adaptive Incremental Kalman Filter," *Sensors*, vol. 17, no. 1, p. 152, Jan. 2017.

[10] M. Liu, Y. Gao, G. Li, X. Guang, and S. Li, "An Improved Alignment Method for the Strapdown Inertial Navigation System (SINS)," *Sensors*, vol. 16, no. 5, p. 621, Apr. 2016.

[11] Arianespace, "ARIANE 5 User's Manual." 2016.

[12] Arianespace, "Vega User's Manual." 2014.

[13] D. H. Titterton and J. L. Weston, *Strapdown inertial navigation technology*, 2nd ed. Reston, USA: American Institute of Aeronautics and Astronautics, 2004.

[14] Y. Yüksel, "Design and Analysis of Transfer Alignment Algorithms," Middle East Technical University, 2005.

[15] W. E. Wiesel, *Modern Orbit Determination*, 2nd ed. Beavercreeck, OH, USA: Aphelion Press, 2010.

[16] M. S. Grewal, L. R. Weill, and A. P. Andrews, *Global Positioning Systems, Inertial Navigation, and Integration*, 2nd ed. Hoboken, NJ, USA: John Wiley & Sons, Inc., 2007.

[17] A. Solimeno, "Low-Cost INS / GPS Data Fusion with Extended Kalman Filter for Airborne Applications," Universidade Técnica de Lisboa, 2007.

[18] E. Süli and D. F. Mayers, *An introduction to numerical analysis*, 1st ed. Cambridge, UK: Cambridge University press, 2003.

[19] N. Trawny and S. I. Roumeliotis, "Technical Report: Indirect Kalman filter for 3D Attitude Estimation," Multiple Autonomous Robotic Systems Laboratory, University of Minnesota, Minneapolis, MN, USA, 2005.

[20] X. Tang, Z. Liu, and J. Zhang, "Square-root quaternion cubature Kalman filtering for spacecraft attitude estimation," *Acta Astronaut.*, vol. 76, no. July 2012, pp. 84–94, Jul. 2012.

[21] S. J. Julier and J. K. Uhlmann, "Unscented Filtering and Nonlinear Estimation," *Proc. IEEE*, vol. 92, no. 3, pp. 401–422, Mar. 2004.

[22] J. F. Kuzanek, "Improved Methods for Computing Drag Corrected Missile Impact," in *Army Science Conference*, 1980, vol. 2, pp. 381–393.